THE JOURNAL OF PHYSICAL CHEMISTRY C LETTERS

2007, *111,* 8407−8409
Published on Web 05/25/2007

Raman Spectral Measuring of the Growth Rate of Individual Single-Walled Carbon Nanotubes

Yagang Yao, Ran Liu, Jin Zhang,* Liying Jiao, and Zhongfan Liu

Center for Nanoscale Science and Technology (CNST), Beijing National Laboratory for Molecular Sciences, Key Laboratory for the Physics and Chemistry of Nanodevices, State Key Laboratory for Structural Chemistry of Unstable and Stable Species, College of Chemistry and Molecular Engineering, Peking University, Beijing 100871, People's Republic of China

Received: April 13, 2007; In Final Form: May 14, 2007

We report, herein, a rational approach to measure the growth rate of individual SWNTs. Intramolecular junctions could be produced controllably by temperature-mediated chemical vapor deposition (CVD) and used as a Raman-identifiable mark to confirm the starting and finishing position of a SWNT. Thus, the growth rate of SWNTs could be calculated by $\nu = L_{CNT}/t$, where ν is the growth rate, L is the length of the segment, and t is its growth time. The results show that the growth rates of SWNTs growing at 950 °C are higher than those at 900 °C, and the growth rate at 950 or 900 °C decreases with the passage of time. We believe this approach provides an easy way to measure the growth rate of an individual SWNT and that it is a good starting point to study the growth behavior of SWNTs and for constructing SWNT-based device.

Single-walled carbon nanotubes (SWNTs) would be an ideal candidate for making the next generation electronic circuits due to its superior electronic and physical properties.[1−4] The critical step in fabricating the full SWNTs' electronic circuit is to grow SWNTs in a controlled manner, during which the growth rate is a crucial issue. A reliable method to measure the growth rate of an individual SWNT will be not only helpful to control the length and locate the site of SWNTs in site-specific and/or aligned growth,[5−11] which is important for the construction of SWNT-based devices, but also instructive to understand the growth mechanism of SWNTs.[5,12−18] By far, nearly all of the methods to measure the growth rates are limited to identifying the beginning and the end of a timed growth,[19−24] and a convincing approach is still being expected.

We report, herein, a rational approach to measure the growth rate of individual SWNTs. Well-separated, orientated, and long SWNTs with controlled intramolecular junctions were grown on a surface[25] by designed temperature-mediated chemical vapor deposition (CVD) using ethanol as the carbon source and $FeCl_3$ or $CoCl_2$ as catalyst precursor (see Supporting Information for details). Using the intramolecular junction as a Raman-identifiable mark (see Figure S2) to confirm the starting and finishing position of the tube growth,[25−29] the growth rate of SWNTs could be calculated by $\nu = L/t$, where ν is the growth rate, L is the length of the segment which can be measured by Raman mapping, and t is its growth time.

As we reported in the last paper, a Raman-identifiable intramolecular junction could be introduced in SWNTs by temperature-mediated CVD.[25] Figure 1a−d shows four typical designed processes to introduce intramolecular junctions in SWNTs in a controlled manner. Processes A (Figure 1a) and B (Figure 1b) were designed to measure the average growth rates of SWNTs catalyzed by the different nanoparticles at the same or different temperatures, while processes C (Figure 1c) and D (Figure 1d) were designed to measure the average growth rates of SWNTs catalyzed by the same catalytic particles at the same or different temperatures.

Figure 1e is a typical scanning electron microscopy (SEM) image of individual SWNTs grown by process A, in which two 1 min temperature oscillations (from 900 to 950 °C and from 950 to 900 °C) were used. As shown in Figure 2a, Raman spectra mapping of the G band indicated that two intramolecular junctions were introduced, and thus, the SWNT was separated into three segments. The growth rate of the second one (shown in light green) can be calculated by $\nu = L/t$. The length of the segment was obtained through SEM and Raman mapping data, and the growth time t was estimated to be about 10−12 min or 20−22 min, according to the length of step II. The growth rate of the six tubes at 950 °C was listed in Figure 2b. Most calculated growth rates are around 5 μm/s, with the highest at 22.4 μm/s and the lowest at 4.5 μm/s. It is evident that the growth rates of the second segments growing at 950 °C in 10 min are generally higher than those at 950 °C in 20 min.

For the process B, the only difference from process A is the direction of the temperature oscillations. The growth rate of the SWNTs growing at 900 °C were obtained and are listed in Figure 2b. Similarly, the growth rates of the second segments growing at 900 °C in 10 min are generally higher than those at

* To whom correspondence should be addressed. Tel. and Fax: 86-10-6275-7157. E-mail: jinzhang@pku.edu.cn.

10.1021/jp072888k CCC: $37.00

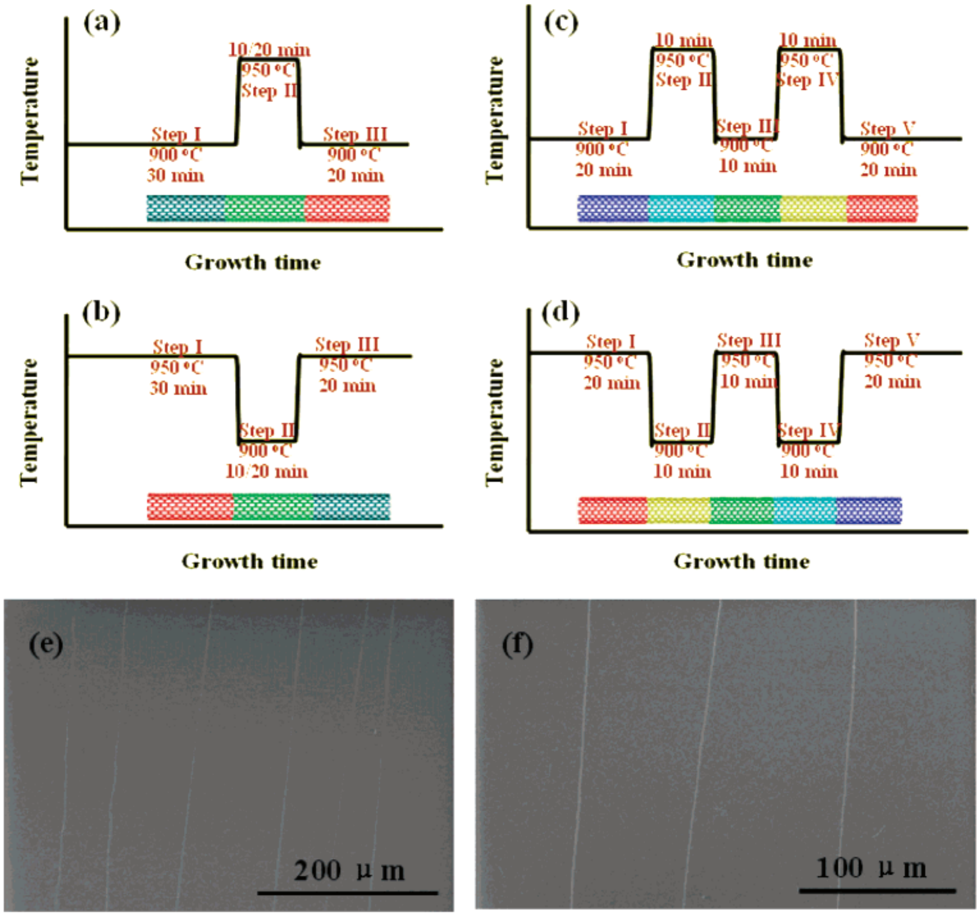

Figure 1. (a), (b), (c), and (d) Schematic diagrams of temperatures and time for the four growth processes A, B, C, and D, respectively. (e) and (f) SEM images of typical growth results.

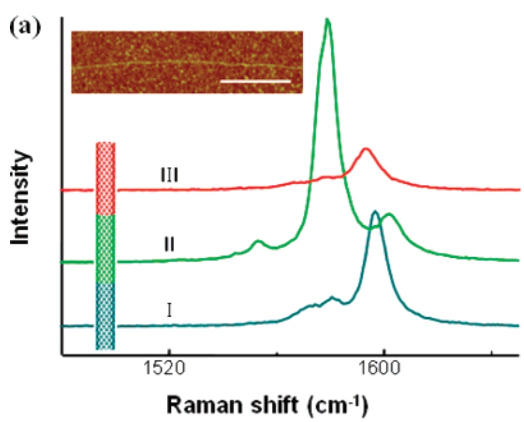

(b)

Process	Tube No.	Temperature [°C]	Growth time [min]	Growth rate [μm/s]
A	1	950	20~22	4.5~4.9
	2			4.9~5.4
	3			4.8~5.2
	4			4.5 ~5.1
	5	950	10~12	18.7~22.4
	6			8.8~10.6
B	7	900	20~22	4.1~4.5
	8			2.9~3.2
	9	900	10~12	4.3~5.2
	10			4.4~5.3

Figure 2. (a) The G-band evolution along tube 3, which consists of three segments (shown in red, light green, and dark green, respectively). The G band along each segment is relatively constant and experiences a sharp shift at the boundary of each of the two segments. The inset in (a) is an atomic force microscopy (AFM) image of tube 3, showing that tube 3 is an individual SWNT. The scale bar is 1 μm. (b) The growth rates of the second segment, which belong to 10 individual ultralong SWNTs in processes A or B.

900 °C in 20 min. Comparing process A with B, it is easy to see that the growth rates of the second segments growing at 950 °C in 10/20 min are generally higher than those at 900 °C in 10/20 min, respectively.

To verify the temperature effect on the growth rate of the same catalyst nanoparticle, processes C and D were designed. Figure 1f is a typical SEM image of SWNTs in which four 1 min temperature oscillations were introduced. Thus, as shown in Figure 3a, Raman spectra mapping of the G band indicated that four intramolecular junctions were produced, and tube 12 (SEM images shown in Figure S1) was separated into five segments. Similarly, the growth rate of the second, third, and fourth ones (shown in sky blue, light green, and yellow, respectively) can be calculated by $\nu = L/t$ (see Figure 3b). Again, the growth time t is about 10−12 min. For process C, most calculated growth rates are around 5 μm/s, with the highest at 8.3 μm/s and the lowest at 0.8 μm/s. It is easy to see that (i) the growth rates of the second and fourth segments growing at

(a)

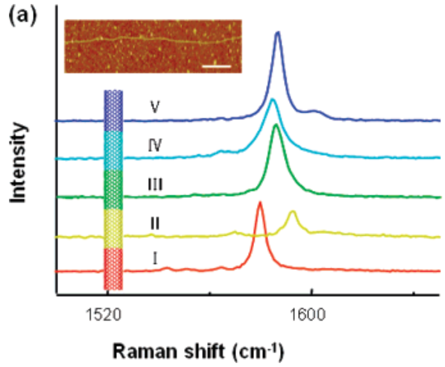

(b)

Process		C				D		
Segment No.		II	III	IV		II	III	IV
Temperature [°C]		950	900	950		900	950	900
Growth time [min]			10~12				10~12	
Growth rate [μm/s]	Tube 11	4.8~5.8	0.8~0.9	3.4~4.1	Tube 13	5.2~6.2	12.1~14.5	1.3~1.6
	Tube 12	6.9~8.3	3.5~4.2	5.6~6.7	Tube 14	8.0~9.6	11.0~13.3	5.0~6.0

Figure 3. (a) The G-band evolution along tube 12, which consists of five segments (shown in dark blue, light blue, light green, yellow, and red, respectively). The G band along each segment is relatively constant and experiences a sharp shift at the boundary of each of the two segments. The inset in (a) is an AFM image of tube 12, showing that tube 12 is an individual SWNT. The scale bar is 1 μm. (b) The growth rates of the second, third, and fourth segments of four individual ultralong SWNTs in processes C or D.

950 °C are higher than that of the third segment growing at 900 °C and (ii) the growth rate at 950 °C decreases with the passage of time, as the growth rate of the fourth segment is lower than that of the second segment.[19] Similar phenomena were also shown in process D.

The correlation between SWNT growth rate, growth temperature, and growth time is consistent with previous work.[19] What is more, the reliability of this approach has been greatly improved. However, the growth rates still have a relative error of −9% (take $t = 10/20$ min as standard). A practical way to improve it is to shorten the temperature oscillations. As is estimated, it takes less than 0.01 s for the formation of the junction, as the AFM data show that the length of the junction is below several nanometers and the growth rates of the SWNTs are about several micrometers per second.[25] If the oscillation could be shortened to 0.1 min and the junctions could still be produced, the growth time of the SWNT segments would be 10−10.1 min or 20−20.1 min. As a result, the relative error of the growth rates would be reduced to less than 1%.

In summary, the growth rates of individual ultralong SWNTs catalyzed by the same or different catalytic nanoparticles at different temperatures were measured by Raman spectroscopy when intramolecular junctions were produced controllably in the growth process as Raman-identifiable marks. Experimental results with good regularities were obtained in our CVD system, indicating that (i) the growth rates of SWNTs growing at 950 °C are higher than those at 900 °C and (ii) the growth rate at 950 or 900 °C decreases with the passage of time. The main cause of the error when the intramolecular junctions were produced during the temperature oscillations is unknown, and the approach can be improved if the time of the temperature oscillation can be shortened.

Acknowledgment. This work was supported by NSFC (20573002, 20673004, 50521201) and MOST (2006CB932701, 2006CB932403).

Supporting Information Available: Experimental details for synthesis of ultralong SWNTs and SWNTs with Raman-identifiable intramolecular junctions by CVD. This material is available free of charge via the Internet at http://pubs.acs.org.

References and Notes

(1) McEuen, P. L. *Nature* **1998**, *393*, 15.
(2) Baughman, R. H.; Zakhidov, A. A.; de Heer, W. A. *Science* **2002**, *297*, 787.
(3) Dai, H. J.; Hafner, J. H.; Rinzler, A. G.; Colbert, D. T.; Smalley, R. E. *Nature* **1996**, *384*, 147.
(4) Rueckes, T.; Kim, K.; Joselevich, E.; Tseng, G. Y.; Cheung, C. L.; Lieber, C. M. *Science* **2000**, *289*, 94.
(5) Huang, L. M.; White, B.; Sfeir, M. Y.; Huang, M. Y.; Huang, H. X.; Wind, S.; Hone, J.; O'Brien, S. *J. Phys. Chem. B* **2006**, *110*, 11103.
(6) Zhang, Y. G.; Chang, A. L.; Cao, J.; Wang, Q.; Kim, W.; Li, Y. M.; Morris, N.; Yenilmez, E.; Kong, J.; Dai, H. J. *Appl. Phys. Lett.* **2001**, *79*, 3155.
(7) Huang, S. M.; Cai, X. Y.; Liu, J. *J. Am. Chem. Soc.* **2003**, *125*, 5636.
(8) Hong, B. H.; Lee, J. Y.; Beetz, T.; Zhu, Y. M.; Kim, P.; Kim, K. S. *J. Am. Chem. Soc.* **2005**, *127*, 15336.
(9) Zhang, Y. Y.; Zhang, J.; Son, H. B.; Kong, J.; Liu, Z. F. *J. Am. Chem. Soc.* **2005**, *127*, 17156.
(10) Kong, J.; Soh, H. T.; Cassell, A. M.; Quate, C. F.; Dai, H. J. *Nature* **1998**, *395*, 878.
(11) Joselevich, E.; Lieber, C. M. *Nano Lett.* **2002**, *2*, 1137.
(12) Louchev, O. A.; Laude, T.; Sato, Y.; Kanda, H. *J. Chem. Phys.* **2003**, *118*, 7622.
(13) Huang, S. M.; Woodson, M.; Smalley, R.; Liu, J. *Nano Lett.* **2004**, *4*, 1025.
(14) Hofmann, S.; Csanyi, G.; Ferrari, A. C.; Payne, M. C.; Robertson, J. *Phys. Rev. Lett.* **2005**, *95*, 036101.
(15) Deng, W. Q.; Xu, X.; Goddard, W. A. *Nano Lett.* **2004**, *4*, 2331.
(16) Ding, F.; Bolton, K.; Rosen, A. *J. Phys. Chem. B* **2004**, *108*, 17369.
(17) He, M. S.; Duan, X. J.; Wang, X.; Zhang, J.; Liu, Z. F.; Robinson, C. *J. Phys. Chem. B* **2004**, *108*, 12665.
(18) Louchev, O. A.; Kanda, H.; Rosen, A.; Bolton, K. *J. Chem. Phys.* **2004**, *121*, 446.
(19) Kim, D. H.; Jang, H. S.; Kim, C. D.; Cho, D. S.; Yang, H. S.; Kang, H. D.; Min, B. K.; Lee, H. R. *Nano Lett.* **2003**, *3*, 863.
(20) Geohegan, D. B.; Puretzky, A. A.; Ivanov, I. N.; Jesse, S.; Eres, G.; Howe, J. Y. *Appl. Phys. Lett.* **2003**, *83*, 1851.
(21) Puretzky, A. A.; Geohegan, D. B.; Jesse, S.; Ivanov, I. N.; Eres, G. *Appl. Phys. A* **2005**, *81*, 223.
(22) Zheng, L. X.; O'Connell, M. J.; Doorn, S. K.; Liao, X. Z.; Zhao, Y. H.; Akhadov, E. A.; Hoffbauer, M. A.; Roop, B. J.; Jia, Q. X.; Dye, R. C.; Peterson, D. E.; Huang, S. M.; Liu, J.; Zhu, Y. T. *Nat. Mater.* **2004**, *3*, 673.
(23) Huang, S. M.; Maynor, B.; Cai, X. Y.; Liu, J. *Adv. Mater.* **2003**, *15*, 1651.
(24) Merkulov, V.; Melechko, A. V.; Guillorn, M. A.; Lowndes, D. H.; Simpson, M. L. *Chem. Phys. Lett.* **2002**, *361*, 492.
(25) Yao, Y. G.; Li, Q. W.; Zhang, J.; Liu, R.; Jiao, L. Y.; Zhu, Y. T.; Liu, Z. F. *Nat. Mater.* **2007**, *6*, 283.
(26) Anderson, N.; Hartschuh, A.; Novotny, L. *Nano Lett.* **2007**, *7*, 577.
(27) Doorn, S. K.; O'Connell, M. J.; Zheng, L. X.; Zhu, Y. T.; Huang, S. M.; Liu, J. *Phys. Rev. Lett.* **2005**, *94*, 016802.
(28) Doorn, S. K.; Zheng, L. X.; O'Connell, M. J.; Zhu, Y. T.; Huang, S. M.; Liu, J. *J. Phys. Chem. B* **2005**, *109*, 3751.
(29) Wu, G.; Dong, J. M. *Phys. Rev. B* **2006**, *73*, 245414.